Journal of proteome research

Article

Cite This: J. Proteome Res. 2019, 18, 1352−1362

pubs.acs.org/jpr

Functional Proteomics of Breast Cancer Metabolism Identifies GLUL as Responder during Hypoxic Adaptation

Stephan Bernhardt,[†] Christian Tönsing,[‡] Devina Mitra,[†] Nese Erdem,[†,§] Karin Müller-Decker,[∥] Ulrike Korf,[†] Clemens Kreutz,[⊥,#] Jens Timmer,[‡,⊥,#] and Stefan Wiemann*[,†,§]

[†]Division of Molecular Genome Analysis, German Cancer Research Center (DKFZ), Im Neuenheimer Feld 580, 69120 Heidelberg, Germany

[‡]Institute of Physics, University of Freiburg, Hermann-Herder-Str. 3, 79104 Freiburg, Germany

[§]Faculty of Biosciences, Heidelberg University, Im Neuenheimer Feld 234, 69120 Heidelberg, Germany

[∥]DKFZ Tumor Models Core Facility, German Cancer Research Center (DKFZ), Im Neuenheimer Feld 280, 69120 Heidelberg, Germany

[⊥]Center for Systems Biology (ZBSA), University of Freiburg, Habsburgerstr. 49, 79104 Freiburg, Germany

[#]CIBSS Centre for Integrative Biological Signalling Studies, University of Freiburg, Schänzlestr. 18, 79104 Freiburg, Germany

Supporting Information

ABSTRACT: Hypoxia as well as metabolism are central hallmarks of cancer, and hypoxia-inducible factors (HIFs) and metabolic effectors are crucial elements in oxygen-compromised tumor environments. Knowledge of changes in the expression of metabolic proteins in response to HIF function could provide mechanistic insights into adaptation to hypoxic stress, tumorigenesis, and disease progression. We analyzed time-resolved alterations in metabolism-associated protein levels in response to different oxygen potentials across breast cancer cell lines. Effects on the cellular metabolism of both HIF-dependent and -independent processes were analyzed by reverse-phase protein array profiling and a custom statistical model. We revealed a strong induction of glucose transporter 1 (GLUT1) and lactate dehydrogenase A (LDHA) as well as reduced glutamate-ammonia ligase (GLUL) protein levels across all cell lines tested as consistent changes upon hypoxia induction. Low GLUL protein levels were correlated with aggressive molecular subtypes in breast cancer patient data sets and also with hypoxic tumor regions in a xenograft mouse tumor model. Moreover, low GLUL expression was associated with poor survival in breast cancer patients and with high HIF-1α-expressing patient subgroups. Our data reveal time-resolved changes in the regulation of metabolic proteins under oxygen-deprived conditions and elucidate GLUL as a strong responder to HIFs and the hypoxic environment.

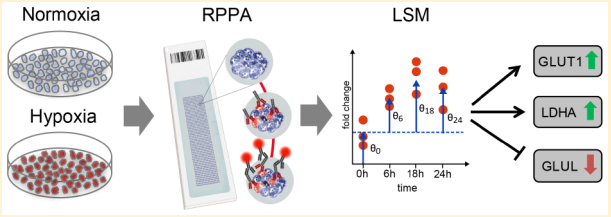

KEYWORDS: *breast cancer, cancer metabolism, GLUL, HIF-1 alpha, hypoxia, protein arrays, RPPA, linear statistical model*

INTRODUCTION

Cancer was recognized as a disease of altered metabolism nearly 100 years ago, but metabolic reprogramming has only recently been documented as an essential hallmark of neoplasia.[1] Furthermore, tumor growth is not only characterized by metabolic adaptation but also by changes in the local microenvironment as well as heterogeneity of the tissue. Diverse cellular differentiation states, for example, in response to oxygen (O_2)-deprived conditions, like hypoxia, can give rise to phenotypically diverse tumors.[2,3] Within a tumor, different levels of perfusion and oxygen are characteristic features of the tissue, and intratumoral hypoxia is characterized as an insufficient oxygen supply for metabolic needs and has been shown to be an independent adverse prognostic factor in many cancers, including breast cancer.[4−6] O_2 deprivation triggers complex adaptive responses at cellular, tissue, and organismal levels to meet the metabolic and bioenergetic demands.[7] The transcription factor hypoxia-inducible factor 1-α (HIF-1α) is the key regulator of the hypoxic response and is induced under hypoxic conditions, thereby leading to adaptation in angiogenesis, invasion/metastasis, as well as substantial metabolic changes in numerous cancer entities.[8] Furthermore, studies support the relation of increased expression of HIF-1α with aggressive tumor growth and poor patient prognosis.[9−12] Along these lines, hypoxic breast tumors do not respond well to established therapeutics, and patients predominantly show worse clinical outcome.[13] Therefore, identifying novel targets driving these hypoxic tumors is a necessary requirement to expand the therapeutic window and to overcome therapy resistance. Moreover, gaining new insights into the adaptation processes under oxygen-deprived conditions will be relevant to

Received: December 10, 2018
Published: January 4, 2019

DOI: 10.1021/acs.jproteome.8b00944
J. Proteome Res. 2019, 18, 1352−1362

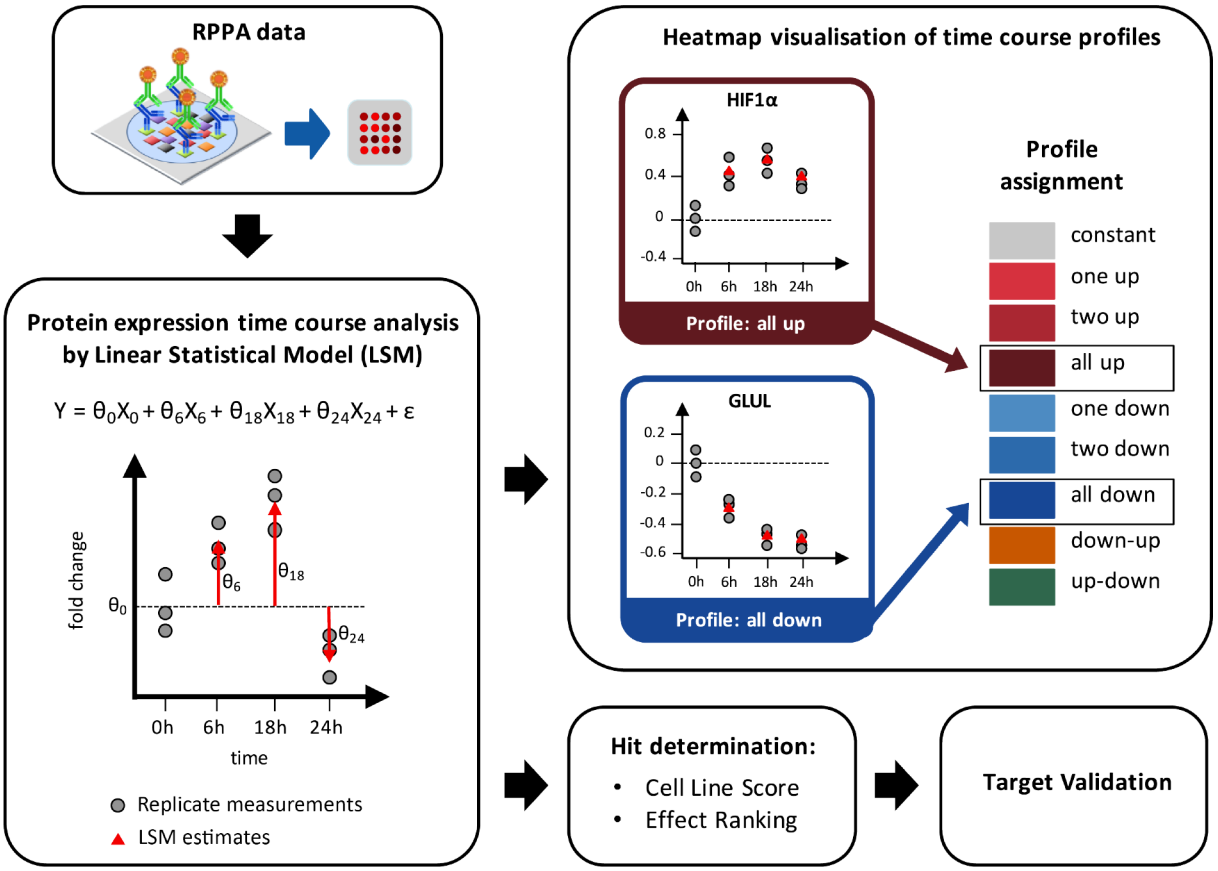

Figure 1. Experimental workflow. Schematic overview of experimental workflow and analysis.

support the development of new stratification regimes, for example, for the optimal selection of breast cancer patients who might benefit from targeted therapies against metabolic proteins for the given microenvironment.

In a previous study, we had analyzed the expression of metabolic proteins in a primary breast cancer cohort and identified prognostic markers.[14] In the present study, we used the same set of metabolic proteins to elucidate time-resolved changes in the regulation of these metabolic proteins in relation to hypoxic conditions. Whereas most research concerning hypoxia and its interaction with the microenvironment has been focused on signaling components at the genome and RNA levels, here we applied an in-depth analysis of time-resolved adaptation of metabolic proteins under various hypoxic conditions to reveal potential drivers of the cancer phenotype. Importantly, mutations in metabolic genes can drive tumorigenesis; more often, however, cancer metabolism is transformed by an altered abundance of the metabolic proteins.[15]

Breast cancer cell lines MCF-7, SKBR3, MDA-MB-231, and MDA-MB-468 were exposed in a time dependent manner to different oxygen conditions (normoxia 21% O_2, mild hypoxia 1.2% O_2, harsh hypoxia 0.2% O_2) and $CoCl_2$ to induce hypoxia-inducible factor (HIF). Then, cell protein lysates were processed via reverse-phase protein arrays (RPPAs), to quantify the levels of 42 metabolism-related proteins. A linear statistical model (LSM) was applied to the data set to determine altered protein expression levels under the given conditions. Subsequent hit determination identified the general and specific protein responses of hypoxic rewiring, providing insight into changes in metabolic protein networks upon HIF and hypoxia induction. The workflow is depicted in Figure 1.

METHODS

Cell Culture

Breast cancer cell lines MCF-7, SKBR3, MDA-MB-231, and MDA-MB-468 were obtained from the American Type Culture Collection ATCC (LGC Standards, Wesel, Germany) and cultivated in RPMI 1640 supplemented with 10% FBS (GIBCO, Darmstadt, Germany). Cell line authentication was performed via multiplex cell line authentication (Multiplexion, Friedrichshafen, Germany), and cell lines were tested for potential contaminations with mycoplasma on a regular basis.

Time-Resolved Perturbation Experiments

Cell lines were routinely maintained under normoxic conditions (5% CO_2, 37 °C, 21% oxygen). To induce oxygen-deprived conditions, cells were incubated at 1.2% oxygen for mild hypoxia (BINDER, Tuttlingen, Germany) or in Anaerocult A mini kit hypoxia bags at 0.2% oxygen (Merck, Darmstadt, Germany) for harsh hypoxic conditions. $CoCl_2$ (Merck) was used at a concentration of 200 μM as a chemical inducer of HIF1. Cells were kept under hypoxic/$CoCl_2$ conditions for 6, 18, or 24 h, before the preparation of protein lysates. Controls were kept in normoxia. In addition, a reoxygenation time point at 26 h (2 h after a 24 h hypoxia/$CoCl_2$ incubation) was taken prior to harvesting. All experiments were performed in biological triplicates.

DOI: 10.1021/acs.jproteome.8b00944
J. Proteome Res. 2019, 18, 1352−1362

Cell Lysis and Sample Preparation

Cells were lysed on ice with ice-cold M-PER lysis buffer (Pierce, Bonn, Germany) containing protease inhibitor Complete Mini and antiphosphatase PhosSTOP (Roche, Mannheim, Germany). Cell lysates were incubated on a tube rotator for 30 min at 4 °C and subsequently centrifuged for 10 min at 16 000*g*. Total protein concentration was quantified with a Pierce BCA protein assay kit according to manufacturer's instructions (Thermo Scientific, Rockford, IL).

Immunoblotting

Protein lysates were denatured using 4× sample loading buffer (Roti-Load 1) for 5 min at 95 °C. Samples were loaded on Mini-PROTEAN TGX precast gels for protein mass separation. After protein separation via SDS-PAGE, the proteins were transferred to a polyvinylidene difluoride membrane (Trans-Blot Turbo LF PVDF membrane) by electrophoresis. The Trans-Blot Turbo transfer system was used for the "semi dry" blotting setup in accordance to the manufacturer's instructions. Membranes were blocked for 1 h at room temperature (RT) with blocking buffer (Rockland Immunochemicals) in TBS (50%, v/v) containing 5 mM NaF and 1 mM Na_3VO_4 and subsequently incubated with target-specific primary antibody overnight at 4 °C on a rocking platform. The membrane was washed 4 × 5 min in TBST, followed by a 1 h incubation with Alexa Fluor 680 conjugated secondary antibody. After washing for 4 × 5 min, the membrane was scanned at an excitation wavelength of 685 nm and a resolution of 84 μm using the Odyssey Infrared Imaging System (Figure S1).

Reverse-Phase Protein Array Profiling

Lysates were adjusted to a total protein concentration of 2 μg/μL, mixed with 4× SDS sample buffer (10% glycerol, 4% SDS, 10 mM DTT, 125 mM Tris−HCl, pH 6.8) and denatured at 95 °C for 5 min. Lysates and dilution series of each cell line, serving as controls, were spotted as technical triplicates on nitrocellulose-coated glass slides (Grace-Biolabs, Bend, OR) using an Aushon 2470 contact spotter (Aushon BioSystems, Billerica, MA). Post spotting, slides were incubated with blocking buffer (Rockland Immunochemicals, Gilbertsville, PA) in TBS (50%, v/v) containing 5 mM NaF and 1 mM Na_3VO_4 for 2 h at room temperature, prior to incubation with target-specific primary antibodies at 4 °C overnight. Primary antibodies had been selected to recognize 42 proteins involved in a wide range of metabolic pathways and to achieve a broad perspective on breast cancer metabolism (Table S1). Antibody validation was carried out as previously described.[16] Primary antibodies were detected with Alexa Fluor 680-coupled goat antimouse IgG or antirabbit IgG in 1:8000 dilutions (Life Technologies, Darmstadt, Germany). In addition, representative slides were stained for total protein quantification using Fast Green FCF protein dye as described before.[17] TIFF images of all slides were obtained at an excitation wavelength of 685 nm and at a resolution of 21 μm using an Odyssey Scanner (LI-COR, St. Lincoln, NE). Signal intensities of individual spots were quantified using GenePixPro 7.0 (Molecular Service, Sunnyvale, CA). Data preprocessing, merging of technical triplicates, background correction, and quality control were performed using the RPPanalyzer R-package.[18]

In Vivo Xenograft Tumors

Animal experiments were performed in accordance with approved guidelines of the local Governmental Committee for Animal Experimentation (RP Karlsruhe, Germany, license G288/14). Mice were maintained at a 12 h light−dark cycle with unrestricted Kliba 3307 diet and tap water. Under isoflurane inhalation anesthesia (1 to 1.5% in O_2, 0.5 L/min), 3 × 10^6 MDA-MB-231 or 2.5 × 10^6 MDA-MB-468 cells suspended in 30 μL of PBS/growth-factor-reduced Matrigel (1:1 v/v for MDA-MB-231 and 3:1 v/v for MDA-MB-468) (BD, Heidelberg, Germany) were injected into the mammary gland fat pad of 8 to 9 week old female NOD SCID gamma (NSG) mice (n = 4 for every xenograft model) recruited from the Center for Preclinical Research (German Cancer Research Center - DKFZ, Heidelberg, Germany). Tumor volume was measured with a caliper and calculated according to the formula: V = (length (mm) × width $(mm)^2$)/2. For stainings, tumors were fixed in 4% paraformaldehyde in PBS and then paraffin-embedded.

Immunohistochemistry

Immunohistochemistry (IHC) was performed on 5 μm FFPE sections. After the blockage of endogenous peroxidases (3% H_20_2 in PBS or Aqua Bidest for 10 min), antigen demasking (0.01 M sodium citrate buffer, pH 6.8, for 10 min (carbonic anhydrase (CA9)) or 20 min (glutamate-ammonia ligase (GLUL)), and blocking in 1% ELISA BSA in PBS (GLUL) or 5% goat serum in TBST (CA9), specimens were stained using primary rabbit antibodies directed against GLUL (1:50 dilution of HPA007316, ATLAS Antibodies, Sigma-Aldrich), CA9 (1:75 dilution of D47G3, Cells Signaling), and secondary antirabbit IgG HRP (111-035-003, diluted 1:200, Dianova, Hamburg, Germany). Nuclei were counterstained with hematoxylin. Sections were analyzed using an Axioskop Microscope System 2 coupled to an Axiocam and Axiovision, rel. 4.3 (Zeiss, Oberkochen, Germany).

Data Analysis

Linear Statistical Model. The preprocessed data of the time courses with triple biological replicates for each time point were analyzed individually for each target protein and treatment. To merge the replicates and assess the direction and strength of regulation over time, a linear statistical model (LSM) was used for the $\log_2$ signal intensities of the target protein time courses. Cook's distance was used to detect outliers in the measured time course.[19,20] On the basis of this, 1% of the data points were removed from the analysis. The basal expression level was determined by the measurements at t = 0 h under 21% O_2 conditions, and was then entered as offset into the LSM. On the basis of this, expression levels under hypoxic and mimic conditions were analyzed over time as fold-change relative to t = 0 h, defining the target protein expression profile. A one-way analysis of variance (ANOVA) was performed on each expression profile to discriminate between a constant time course signal at the basal expression level of the target protein and significantly regulated expression profiles (p < 0.05). Using t-statistics, the time-point-specific regulation estimates of the LSM were tested individually against the respective basal expression estimate to identify significantly regulated proteins (p < 0.05). All p values were FDR-adjusted for multiple tests using the Benjamini−Hochberg procedure.[21]

Determination of Expression Profiles. To detect differential expression profiles in 504 time courses, the p values of the ANOVA and the LSM estimates were used.

DOI: 10.1021/acs.jproteome.8b00944
J. Proteome Res. 2019, 18, 1352−1362

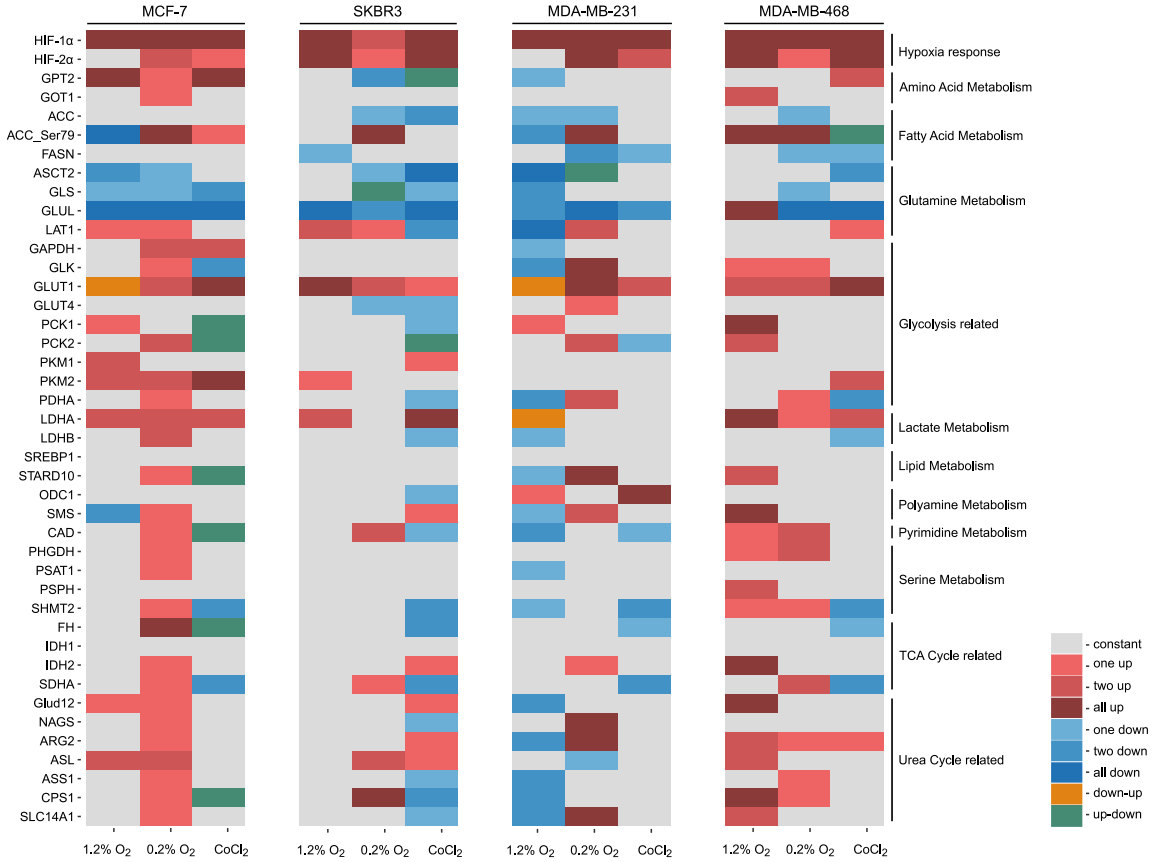

Figure 2. Heatmap visualization of protein time course profiles. The heatmap represents the condensed time course data of each protein target on the basis of the linear statistical model results. Nonsignificantly regulated proteins revealing constant expression at the level of normoxic condition are labeled in gray. Red and blue tiles indicate significantly up- or down-regulated proteins, respectively. Dark colors indicate higher occurrences of corresponding regulations in the LSM results. Expression profiles with alternating sign of significant regulations are labeled in orange and green. $CoCl_2$, cobalt chloride; TCA, tricarboxylic acid cycle.

Profiles without any indication of significant regulation in either of the two tests were considered as constant profiles, that is, without regulation relative to the basal protein expression level under 21% O_2 conditions. Significant regulation indicated by an FDR-adjusted p value <0.05 of the t-statistics for at least one LSM estimate of the perturbed conditions was linked to up- or down-regulation depending on the sign of the LSM estimate. Time courses with one, two, or three significantly up-regulated time points were assigned to expression profiles "one up", "two up", and "all up", respectively, and likewise for down-regulated signals. Expression profiles with alternating sign, for example, a significant down-regulation followed by a nonsignificant regulation and further by a significant up-regulation, were specified as "down−up", whereas the opposite was termed as "up−down".

Ranking of Protein Profiles. A Cell Line (CL) score in the range from 0 to 4 was assigned to all target proteins for each treatment to quantify the significantly nonconstant expression profile behavior through all cell lines. We defined this score such that a CL score of 0 indicates target proteins that are not significantly regulated in any cell line, whereas a CL score of 1 indicates significantly regulated time courses in one cell line, a CL score of 2 in two cell lines, a CL score of 3 in three cell lines and a CL score of 4 in all four cell lines.

As a second indicator for the key regulated proteins over time, the Effect Ranking (EF) was defined for the strength of regulation given by individual fold changes. For this, target profiles were ranked by their maximal regulation strength over all time points in the expression profile as well as by the squared sum of residuals (SSRs) from the ANOVA, in both cases individually for each cell line and treatment combination. Both series were merged by the Rank Product, resulting in the EF.[22] Furthermore, the "rank per treatment" was determined by another Rank Product combination of the EFs from all cell lines individually for each treatment. By analogy, the "overall rank" was constructed as a comprehensive combination of all EFs, first from all cell lines and second over all treatments, using the Rank Product, respectively.

TCGA and METABRIC Data Analysis. Publicly available RNA-sequencing data and clinical annotations of primary breast cancer tumors were obtained from The Cancer Genome Atlas (TCGA).[23] Level 3 normalized gene expression data of that cohort (TCGA_BRCA_exp_HiSeqV2-2015-02-24) were downloaded from the cBioPortal Web site.[24,25] Data on gene expression and clinical characteristics of primary breast cancer tumors were publicly available (EGAS00000000083) from the Molecular Taxonomy of Breast Cancer International Consortium (METABRIC).[26] Gene expression data were $\log_2$-transformed and subset to the genes of interest. Patient data were subjected to Kaplan−Meier analysis of overall survival (OS) and recurrence-free survival (RFS). Differences in Kaplan−Meier curves were statistically tested using the log-rank test. Differences between subgroups depicted in the boxplots were analyzed with unpaired Student's t test for two-

DOI: 10.1021/acs.jproteome.8b00944
J. Proteome Res. 2019, 18, 1352−1362

group comparison or ANOVA for multiple groups, as indicated in the Figure legends, respectively. For tumor stage comparison, patients were grouped based on the TNM staging guidelines.[27] T1 refers to all low-stage breast cancer patients determined as T1. T2+ refers to all higher stage patients determined as T2 and higher (T2, T3, and T4).

Data were analyzed using GraphPad Prism 5 (La Jolla, CA) or the R statistical computing environment (version 3.2.2).[28] A p value <0.05 was considered as statistically significant.

RESULTS AND DISCUSSION

RPPA Profiling

In total, four cell lines, each grown under normoxic (21% O_2), mild hypoxic (1.2% O_2), oxygen-deprived (0.2% O_2), and $CoCl_2$ conditions, were analyzed in three biological replicates and at five time points (time point 0 h in normoxic conditions, time points 6, 18, and 24 h after incubation under hypoxic/$CoCl_2$ conditions, and time point 26 h after 2 h of reoxygenation). Cell lysates were spotted in technical triplicates to produce RPPA arrays, and 42 proteins were quantified to generate a final data set composed of 7560 data points. The preprocessed RPPA data are presented in Table S2.

Heatmap Visualization of the Data Set via a Linear Statistical Model of Time Courses

A heatmap approach tailored to the design of the data set was applied to the proteomic time-course data to distinguish between constant protein expression patterns and significantly regulated proteins upon hypoxia treatment over time compared with the respective normoxic condition. Along these lines, ANOVA and t-statistics on the LSM estimates were used to categorize individual protein expression time courses and enable visualization (Figure S2). The 504 protein expression time courses were then visualized in a heatmap (Figure 2).

HIF-1α, the main regulator of oxygen homeostasis, is known to be upregulated under oxygen-deprived conditions in mammalian cells and to regulate a variety of genes.[29,30] Consistent with this function, protein levels of HIF-1α were significantly upregulated under all hypoxic as well as $CoCl_2$ conditions and in all cell lines tested, validating our experimental approach. Furthermore, hypoxia-inducible factor 2 alpha (HIF-2α), another subunit of HIF-α, responsible for driving the chronic hypoxic response (>24 h), showed just a partial upregulation under the given conditions across all time points and cell lines tested, validating its different mode of regulation.[31]

The vast majority of metabolic enzymes analyzed did not show consistent patterns in their respective expression levels upon treatment over time and across cell lines. Rather, the response patterns during oxygen deprivation pointed toward cell-line-specific effects as the most prominent feature, likely reflecting the heterogeneous nature of metabolic activities in the respective cell lines. Furthermore, proteomic and metabolic differences within all cell lines might result in a different adaptation to oxygen deprivation. The presence of heterogeneous metabolic profiles rather than a universal metabolic pattern in cell lines and cancer entities has been reported before.[32] Along these lines, our findings reveal heterogeneity under oxygen-deprived conditions, as we found individual proteins to be affected upon hypoxia exposure primarily in particular cell lines. For example, arginase 2 (ARG2) was significantly upregulated over time and under all conditions in the basal-like MDA-MB-468 cell line, whereas pyruvate kinase M2 (PKM2) was significantly upregulated in the luminal cell line MCF-7. These findings are in line with prior knowledge of a direct role for HIFs in mediating PKM2 and ARG2 expression based on tumor cell entity and breast cancer subtype.[33−36]

In addition, we employed $CoCl_2$, a mimic of hypoxia that activates HIF-1α also under normoxic conditions, to differentiate between HIF-1α-dependent and -independent processes.[37,38] Only a few proteins (e.g., SDHA and FH) were significantly altered in expression over time by $CoCl_2$ treatment only, as compared with physiological hypoxia, indicating different HIF-1α- and hypoxia dependent regulations. Some proteins (e.g., IDH1) showed no significant changes in expression upon hypoxia or hypoxia-mimicking conditions across all cell lines tested, resulting in constant protein levels. Glucose transporter 1 (GLUT1), a known maker of hypoxia and regulated by HIF, was consistently upregulated, whereas other proteins (e.g., GLUL) were mostly downregulated in all given treatments and cell lines tested, representing possible general responders to hypoxic conditions.[39,40]

GLUT1, LDHA, and GLUL Are Regulated by the HIF-Driven Hypoxic Response

To verify individual candidates, the CL score was introduced, revealing significantly regulated proteins (independent of the direction of regulation) over all investigated cell lines and for each applied condition (Figure 3).

As highlighted in Figure 3, protein expression changes of HIF-1α, GLUT1, and GLUL stood out with maximum CL scores across all conditions tested.

Next, we applied the EF, which quantifies the magnitude of regulation during treatment compared with the respective basal

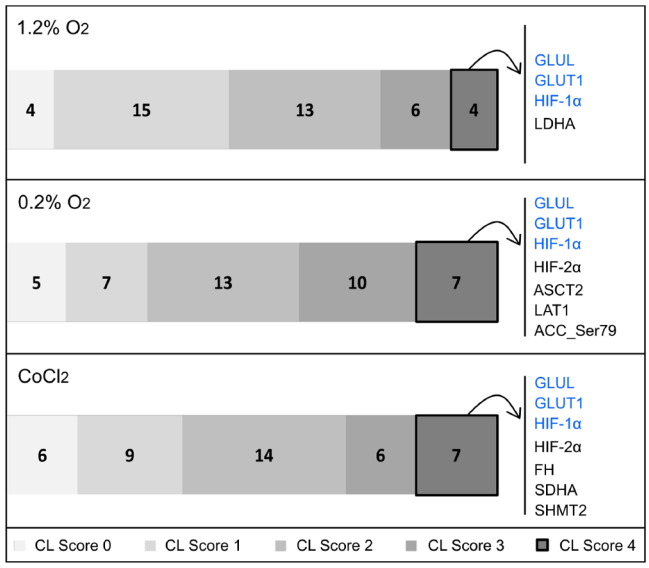

Figure 3. Cell Line score results. Illustrated are the results from the Cell Line (CL) score analysis. A CL score of 0 indicates proteins that are not significantly regulated in any cell line, whereas a CL score of 1 indicates significantly regulated protein time courses in one cell line, a CL score of 2 in two cell lines, a CL score of 3 in three cell lines, and a CL score of 4 in all four cell lines. The full list of proteins and their respective CL scores for each condition are represented in Table S3.

DOI: 10.1021/acs.jproteome.8b00944
J. Proteome Res. 2019, 18, 1352−1362

Table 1. Rank Product Results[a]

target	overall rank	rank per treatment			affiliation
		1.2% O_2	0.2% O_2	$CoCl_2$	
HIF-1α	1	1	1	1	hypoxia response
GLUT1	2	3	3	5	glycolysis-related
LDHA	3	2	8	4	lactate metabolism
GLUL	4	5	9	2	glutamine metabolism
HIF-2α	5	10	5	3	hypoxia response
LAT1	6	4	4	12	glutamine metabolism
ACC_Ser79	7	8	2	23	fatty acid metabolism
PCK1	8	6	20	6	glycolysis-related
ASCT2	9	9	17	8	glutamine metabolism
CAD	10	19	10	7	pyrimidine metabolism
GLK	11	11	6	28	glycolysis-related
PDHA	12	16	12	18	glycolysis-related
IDH2	13	22	11	17	TCA-cycle-related
GLS	14	26	7	21	glutamine metabolism
GPT2	15	21	16	10	amino acid metabolism
SMS	16	7	23	24	polyamine metabolism
SDHA	17	n.s.	22	9	TCA-cycle-related
PKM2	18	13	18	14	glycolysis-related
CPS1	19	28	14	15	urea-cycle-related
GAPDH	20	12	19	22	glycolysis related
SHMT2	21	17	37	11	serine metabolism
ARG2	22	29	13	27	urea-cycle-related
PCK2	23	27	27	13	glycolysis-related
GOT1	24	14	25	n.s.	amino acid metabolism
PSAT1	25	15	24	n.s.	serine metabolism
PKM1	26	18	n.s.	20	glycolysis-related
FH	27	n.s.	33	16	TCA-cycle-related
FASN	28	n.s.	15	32	fatty acid metabolism
Glud12	29	20	28	30	urea-cycle-related
NAGS	30	33	21	25	urea-cycle-related
ODC1	31	31	n.s.	19	polyamine metabolism
ASL	32	24	36	29	urea-cycle-related
STARD10	33	25	29	34	lipid metabolism
LDHB	34	23	31	35	lactate metabolism
ASS1	35	35	26	26	urea-cycle-related
GLUT4	36	n.s.	30	33	glycolysis-related
SLC14A1	37	32	34	36	urea-cycle-related
ACC	38	34	35	31	fatty acid metabolism
PSPH	39	30	n.s.	n.s.	serine metabolism
PHGDH	40	n.s.	32	n.s.	serine metabolism
SREBP1	n.s.	n.s.	n.s.	n.s.	lipid metabolism
IDH1	n.s.	n.s.	n.s.	n.s.	TCA-cycle-related

[a]n.s.: not significant.

protein expression levels under the normoxic conditions, for both transient and sustained expression profiles. In agreement with the CL score, HIF-1α, GLUT1, GLUL, as well as lactate dehydrogenase A (LDHA) presented the highest "overall ranks" (Table 1).

Furthermore, along with our initial observations, protein expression of GLUT1 and LDHA was significantly elevated under hypoxic conditions, and GLUL protein expression levels were significantly down-regulated. Taken together, out of all proteins investigated, CL score and EF confirmed GLUT1 and GLUL as the most affected metabolic proteins in regard to their significant hypoxic response at the proteomic level and across all four considered cell lines as well as treatments applied, emphasizing the importance of these proteins during hypoxia. Consequently, we hypothesized that these protein expression patterns might indicate a more general mechanism that could be relevant in several subtypes of hypoxic breast cancer. Indeed, HIF-1α stabilization in response to environmental factors like hypoxia contributes in many ways to a pro-growth, glycolytic metabolic program by synchronizing proliferation rates with O_2 availability.[41] Concomitantly, HIF-1α is known to be an important contributor to the Warburg effect by inducing the expression of many genes, including several encoding glycolytic enzymes, like GLUT1 and LDHA.[42−44] Moreover, the conversion of pyruvate to lactate and its removal by lactate transporters allows cancer cells to regenerate NAD^+ and to maintain the glycolytic flux in hypoxia.[45] Furthermore, the promotion of lactate production by HIF-1α is a phenomenon that has been suggested to promote survival in hypoxic settings.[46] Our findings are thus

DOI: 10.1021/acs.jproteome.8b00944
J. Proteome Res. 2019, 18, 1352−1362

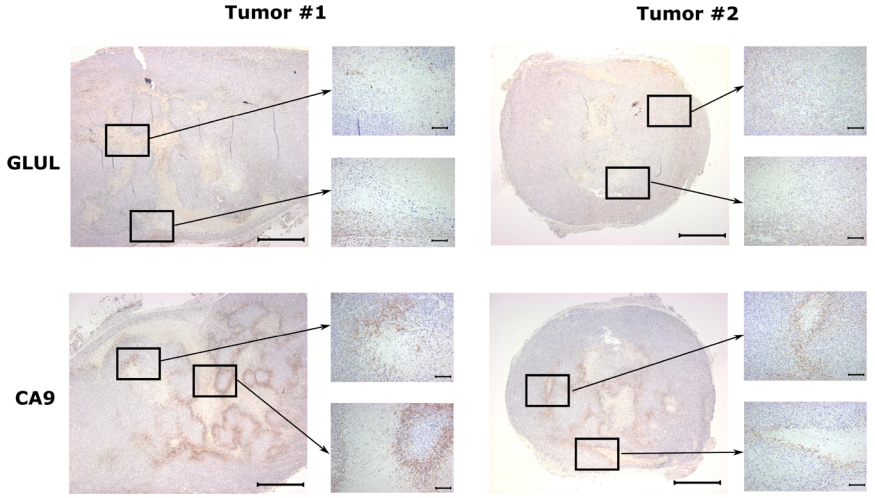

Figure 4. GLUL protein expression in MDA-MB-231 xenograft tumors is confined to the oxygenized tumor periphery. Immunohistochemical staining of GLUL and carbonic anhydrase 9 (CA9) protein expression in sections from two xenograft tumors. Bars: 1000 μm (whole tumor images), 100 μm (inserts).

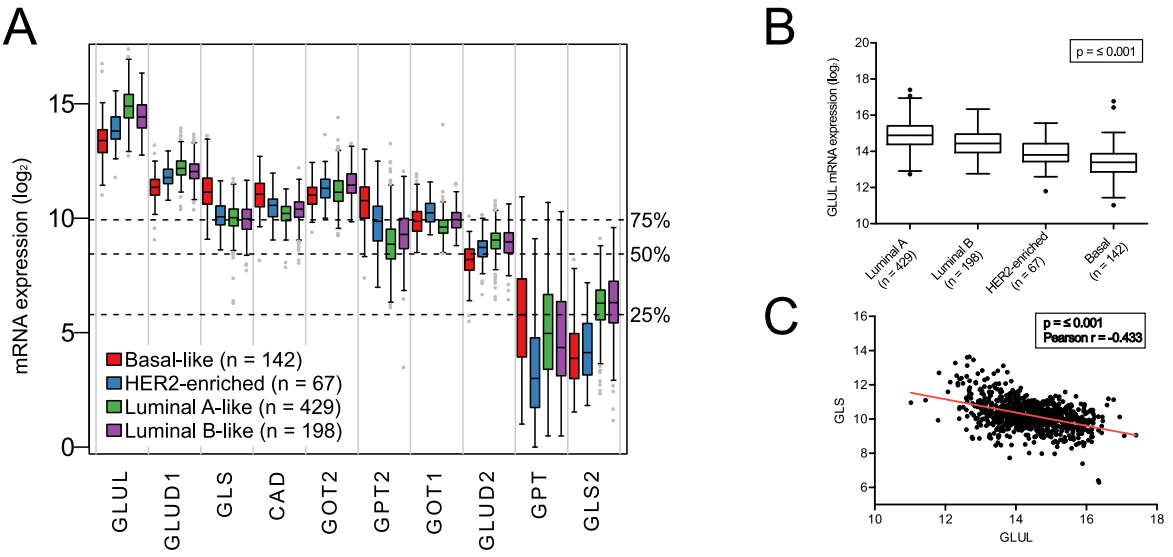

Figure 5. GLUL expression profile. Boxplots represent TCGA data of *GLUL* mRNA expression in comparison with other glutamine-related genes (A) and in detail across different breast cancer subtypes (B). Pearson correlation of *GLS* and *GLUL* mRNA expression is presented in panel C. Statistical difference in groups was tested with ANOVA. p, *p* value; r, Pearson correlation coefficient.

consistent with previous studies reporting a substantial shift toward anaerobic glycolysis as the major metabolic feature of HIF-1α stabilization.[47]

Down-regulation of GLUL under oxygen-deprived conditions would support the switch of breast cancer cells to glycolysis for energy production; therefore, we further focused on the novel connection of hypoxia and the glutamine-producing enzyme GLUL in breast cancer. Interestingly, glutaminase (GLS) protein expression, responsible for the reverse reaction of GLUL by generating glutamate out of glutamine, was not found to be continually significantly regulated during hypoxic treatment in the cell lines, except in MCF7. Whereas GLS is widely known as an important regulator of glutamine metabolism, few studies have focused on GLUL as a potential determinant of glutamine homeostasis, especially under hypoxic conditions.[48]

GLUL Tumor Expression in Vivo

Whereas the critical role of glutamine metabolism has been well established in cancer, it is less clear how important the levels of glutamine-producing enzyme GLUL and glutamine itself are in tumors that often encounter nutrient and oxygen shortages.[49] An important aspect of hypoxia is the diverse distribution of oxygen-deprived areas within tumors. Furthermore, poor vasculature of tumors remains a challenge because conventional chemotherapeutic agents as well as radiation are less effective in oxygen-deprived cells.[50,51] Using MDA-MB-231 and MDA-MB-468 cell lines in xenograft tumor models of triple-negative breast cancer, we thus investigated the spatial distribution of expression of GLUL as well as hypoxic marker carbonic anhydrase within xenograft tumors (Figure 4).

IHC for GLUL and carbonic anhydrase (CA9) showed mutual exclusivity of expression, which is fully in line with the in vitro findings we made in the proteomic experiment. The

DOI: 10.1021/acs.jproteome.8b00944
J. Proteome Res. 2019, 18, 1352−1362

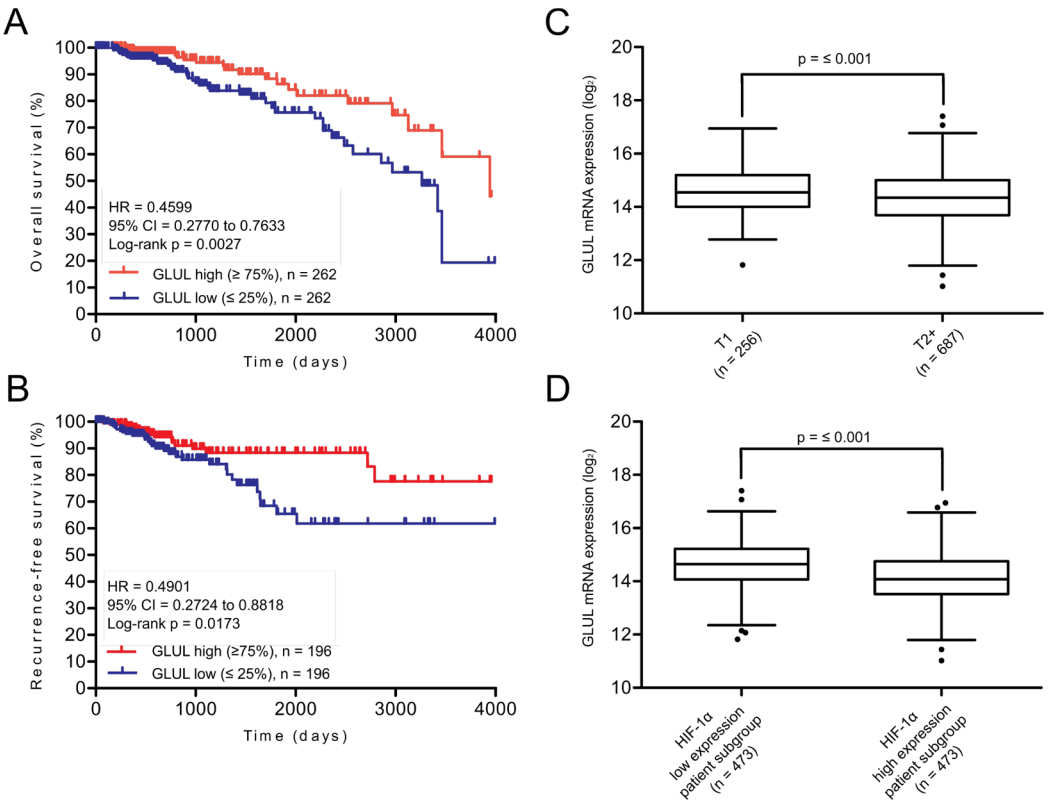

Figure 6. Kaplan−Meier survival estimates of *GLUL* mRNA expression and boxplot representation of T stage and HIF1-α association. TCGA data set was used for Kaplan−Meier plots of *GLUL* mRNA expression for overall survival (OS) (A) and recurrence-free survival (RFS) (B). Patients were grouped based on their mRNA expression with GLUL high defined as the 25% of patients showing the highest GLUL mRNA expression and GLUL low representing the 25% of the patients showing the lowest GLUL expression. Statistical difference in outcome between high and low gene expression were compared by log-rank test. Boxplots represent *GLUL* mRNA expression in association to T stage (C) and HIF1-α expression subgroups (D). CI, confidence interval; HR, hazard ratio; p, *p* value.

IHC data suggest that whereas GLUL indeed seems to be negatively regulated by hypoxia, this is likely not a direct effect of HIF-1α, which has been reported to rather induce gene expression by binding to regulatory sequences in respective target genes.[42] Whereas carbonic anhydrase mostly stained cells in the periphery of necrotic areas within the tumors, GLUL expression was particularly high at the tumor rim as well as in other regions of the tumors showing low carbonic anhydrase expression. These patterns of GLUL and carbonic anhydrase expression were consistently observed in both xenograft models (Figure 4) and are concordant with reduced GLUL expression levels that were detected in vitro upon the induction of hypoxic conditions in our proteomic data set. These findings corroborate the concept of oxygen levels depending on the morphology of tumors, with harsh hypoxic areas presenting toward the necrotic tumor center and validating downregulation of GLUL seen upon hypoxia also at the in vivo level.[52]

Differential Expression of GLUL in Primary Human Breast Cancers

Having identified GLUL as one of the top-regulated proteins in our data set, we further tested the correlation of *GLUL* mRNA expression in breast cancer (BC) patients and subtypes.

Using data from TCGA, *GLUL* mRNA expression was found to be highest among all glutamine-related genes analyzed (Figure 5A), in line with the role of GLUL in glutamine anabolism.[23] Furthermore, *GLUL* gene expression was significantly different between BC subtypes and found to be elevated particularly in luminal compared with the more aggressive basal-like and HER2 breast cancer subtypes, suggesting higher de novo glutamine synthesis via GLUL in the luminal subtype and supporting studies addressing the fact that different cancer subtypes display distinct patterns of glutamine metabolism (Figure 5B).[53] Moreover, basal-like breast tumors have previously been shown to be more hypoxic than luminal tumors supporting the link between hypoxia and low GLUL protein expression.[54,23,55,56] In addition, studies in human BC cells demonstrate that estrogen-receptor-positive BC cell lines are less dependent on extracellular glutamine than triple-negative breast cancer cell lines.[57,58] Along these lines, a report on primary estrogen-receptor-negative breast tumors shows a high glutamate/glutamine ratio, indicating increased glutamine catabolism.[59] Furthermore, the distribution of GLUL in BC subtypes showed a significant inverse association with GLS expression, an enzyme that catalyzes the reverse reaction of GLUL (Figure 5C). GLS is reported to be the main mediator of glutaminolysis in normoxia and is primarily regulated through MYC activation.[60,61] However, GLS was not represented among the top regulated proteins in our data set, highlighting GLUL as a prominent responder of the rewiring of glutamine metabolism in a hypoxic setting.

Fluctuations in hypoxia have been observed in tumors and have been shown to result in higher levels of stabilized HIF-1α compared with continuous hypoxia,[62] and ammonia may directly or indirectly lead to HIF-1α stabilization.[63] These findings support the observed low GLUL levels in hypoxia

DOI: 10.1021/acs.jproteome.8b00944
J. Proteome Res. 2019, 18, 1352−1362

given that GLUL uses ammonia to produce glutamine out of glutamate.

GLUL Expression Is Associated with Survival and HIF-1α Expression in Breast Cancer Patients

Finally, we assessed the potential prognostic value of GLUL expression on RFS and OS in BC patients as well as its expression in subgroups of patients with different HIF1-α levels.

Kaplan−Meier survival estimates revealed a significant difference between patients with high and low *GLUL* mRNA expression in both RFS (p = 0.0173, Figure 6B) and OS (p = 0.0027, Figure 6A). High *GLUL* mRNA expression was associated with a more favorable RFS and OS. Along these lines, lower *GLUL* mRNA expression was also significantly correlated with a higher Tumor (T) stage (Figure 6C). In the context of hypoxia, we examined *GLUL* mRNA expression in high versus low *HIF-1α*-expressing patient groups and found a significant association of low *GLUL* expression with high-*HIF-1α*-expressing breast cancer patients, further supporting our initial results showing a negative correlation between HIF-1α and GLUL levels (Figure 6D).

These observations were additionally confirmed in another independent breast cancer data set (METABRIC) and thus support the relevance of GLUL as a potential prognostic factor in breast cancer as well as a potential responder of the HIF-driven hypoxic rewiring in breast tumors (Figure S3).[26]

CONCLUSIONS

Cancer therapy based on perturbing metabolic pathways will require both knowledge of mechanisms that are employed in the presence of oxygen and insights into the metabolic rewiring in the absence of oxygen. Apart from revealing metabolic proteins significantly affected during hypoxic adaptation, identifying main responders of oxygen deprivation, like GLUL, leads to a better understanding of the hypoxic phenotype and may facilitate more precise diagnosis, better stratification regimes, and improved prognosis predictions of cancer patients. Our results not only confirm that HIF-1α protein expression functions canonically as glycolytic regulator but also suggest a role of hypoxia in glutamine metabolism via GLUL. Screening tumor extracts for relevant hypoxic signatures could thus be a first step toward identifying appropriate stratification regimes of hypoxic tumors. Therefore, further studies of GLUL and its association with hypoxic conditions as well as investigating the possible utility of GLUL as a hypoxia marker in breast cancer patients could be a promising approach.

ASSOCIATED CONTENT

Supporting Information

The Supporting Information is available free of charge on the ACS Publications website at DOI: 10.1021/acs.jproteome.8b00944.

Figure S1. Western Blot representation of GLUL and HIF1-α. Figure S3. Kaplan−Meier survival estimates and boxplot representation of GLUL mRNA expression as well as HIF1-α association (PDF)

Figure S2. Time-course data and LSM results of protein targets (PDF)

Table S1. Antibody list. Table S2. RPPA expression data. Table S3. CL score results (XLSX)

AUTHOR INFORMATION

Corresponding Author

*Tel: +49 6221 42 4702. Fax: +49 6221 42 3454. E-mail: s.wiemann@dkfz.de.

ORCID

Christian Tönsing: 0000-0003-2822-5191

Author Contributions

S.B., C.T., and U.K. conceived concept and design of the study; S.B. and D.M. carried out the experimental work; S.B., C.T, C.K., J.T., and S.W. carried out analysis and interpretation of data; S.B. and C.T. performed bioinformatic and statistical analyses; N.E. and K.M-D. carried out xenograft experiments; S.B. and C.T. prepared figures and tables; and S.B. and S.W. carried out the drafting of manuscript. All authors have given approval to the final version of the manuscript.

Notes

The authors declare no competing financial interest.

ACKNOWLEDGMENTS

We acknowledge Maria Llamazares Prada and Peter Angel for their assistance and provision of experimental material and facilities. Support by the DKFZ Light Microscopy Facility is gratefully acknowledged. This work was supported by the German Federal Ministry of Education and Research (e:Med − FKZ: 031A429; e:Bio − FKZ: 0316168, 031A429, and 0316173; EA:Sys − FKZ 031L0080) and the European Union's Horizon 2020 research and innovation program under the Marie Skłodowska-Curie grant agreement (Epi-Predict − 642691). All of these study sponsors have no roles in the study design, the collection, the analysis, and the interpretation of data.

ABBREVIATIONS

ANOVA, analysis of variance; BC, breast cancer; CL, cell line score; CI, confidence interval; EF, effect ranking; FDR, false discovery rate; HR, hazard ratio; HR+, hormone-receptor-positive; HR−, hormone-receptor-negative; ID, identifier; LSM, linear statistical model; METABRIC, Molecular Taxonomy of Breast Cancer International Consortium; n.s., not significant; OS, overall survival; RFS, recurrence-free survival; RPPA, reverse-phase protein array; TCGA, The Cancer Genome Atlas network

REFERENCES

(1) Hanahan, D.; Weinberg, R. A. Hallmarks of Cancer: The next Generation. *Cell* **2011**, *144* (5), 646−674.

(2) Bertos, N. R.; Park, M. Breast Cancer - One Term, Many Entities? *J. Clin. Invest.* **2011**, *121* (10), 3789−3796.

(3) Pinder, S. E.; Ellis, I. O. The Diagnosis and Management of Pre-Invasive Breast Disease: Ductal Carcinoma in Situ (DCIS) and Atypical Ductal Hyperplasia (ADH)−Current Definitions and Classification. *Breast Cancer Res.* **2003**, *5* (5), 254−257.

(4) Brown, N. S.; Bicknell, R. Hypoxia and Oxidative Stress in Breast Cancer: Oxidative Stress: Its Effects on the Growth, Metastatic Potential and Response to Therapy of Breast Cancer. *Breast Cancer Res.* **2001**, 3 (5), 323−327.

(5) Vaupel, P. Prognostic Potential of the Pre-Therapeutic Tumor Oxygenation Status. *Adv. Exp. Med. Biol.* **2009**, *645*, 241−246.

(6) McKeown, S. R. Defining Normoxia, Physoxia and Hypoxia in Tumours-Implications for Treatment Response. *Br. J. Radiol.* **2014**, *87* (1035), 20130676.

DOI: 10.1021/acs.jproteome.8b00944
J. Proteome Res. 2019, 18, 1352−1362

(7) Lee, K. E.; Simon, M. C. SnapShot: Hypoxia-Inducible Factors. *Cell* **2015**, *163* (5), 1288−1288.e1.
(8) Vaupel, P.; Mayer, A. Hypoxia in Cancer: Significance and Impact on Clinical Outcome. *Cancer Metastasis Rev.* **2007**, *26* (2), 225−239.
(9) Chen, L.; Shi, Y.; Yuan, J.; Han, Y.; Qin, R.; Wu, Q.; Jia, B.; Wei, B.; Wei, L.; Dai, G.; et al. HIF-1 Alpha Overexpression Correlates with Poor Overall Survival and Disease-Free Survival in Gastric Cancer Patients Post-Gastrectomy. *PLoS One* **2014**, *9* (3), e90678.
(10) Baba, Y.; Nosho, K.; Shima, K.; Irahara, N.; Chan, A. T.; Meyerhardt, J. A.; Chung, D. C.; Giovannucci, E. L.; Fuchs, C. S.; Ogino, S. HIF1A Overexpression Is Associated with Poor Prognosis in a Cohort of 731 Colorectal Cancers. *Am. J. Pathol.* **2010**, *176* (5), 2292−2301.
(11) Kurokawa, T.; Miyamoto, M.; Kato, K.; Cho, Y.; Kawarada, Y.; Hida, Y.; Shinohara, T.; Itoh, T.; Okushiba, S.; Kondo, S.; et al. Overexpression of Hypoxia-Inducible-Factor 1alpha(HIF-1alpha) in Oesophageal Squamous Cell Carcinoma Correlates with Lymph Node Metastasis and Pathologic Stage. *Br. J. Cancer* **2003**, *89* (6), 1042−1047.
(12) Zhou, J.; Huang, S.; Wang, L.; Yuan, X.; Dong, Q.; Zhang, D.; Wang, X. Clinical and Prognostic Significance of HIF-1α Overexpression in Oral Squamous Cell Carcinoma: A Meta-Analysis. *World J. Surg. Oncol.* **2017**, *15* (1), 104.
(13) Rapisarda, A.; Melillo, G. Overcoming Disappointing Results with Antiangiogenic Therapy by Targeting Hypoxia. *Nat. Rev. Clin. Oncol.* **2012**, *9* (7), 378−390.
(14) Bernhardt, S.; Bayerlová, M.; Vetter, M.; Wachter, A.; Mitra, D.; Hanf, V.; Lantzsch, T.; Uleer, C.; Peschel, S.; John, J.; et al. Proteomic Profiling of Breast Cancer Metabolism Identifies SHMT2 and ASCT2 as Prognostic Factors. *Breast Cancer Res.* **2017**, *19*, 112.
(15) DeBerardinis, R. J.; Thompson, C. B. Cellular Metabolism and Disease: What Do Metabolic Outliers Teach Us? *Cell* **2012**, *148* (6), 1132−1144.
(16) Henjes, F.; Bender, C.; von der Heyde, S.; Braun, L.; Mannsperger, H. A.; Schmidt, C.; Wiemann, S.; Hasmann, M.; Aulmann, S.; Beissbarth, T.; et al. Strong EGFR Signaling in Cell Line Models of ERBB2-Amplified Breast Cancer Attenuates Response towards ERBB2-Targeting Drugs. *Oncogenesis* **2012**, *1* (7), e16.
(17) Loebke, C.; Sueltmann, H.; Schmidt, C.; Henjes, F.; Wiemann, S.; Poustka, A.; Korf, U. Infrared-Based Protein Detection Arrays for Quantitative Proteomics. *Proteomics* **2007**, *7* (4), 558−564.
(18) Mannsperger, H. A.; Gade, S.; Henjes, F.; Beissbarth, T.; Korf, U. RPPanalyzer: Analysis of Reverse-Phase Protein Array Data. *Bioinformatics* **2010**, *26* (17), 2202−2203.
(19) Cook, R. D. Detection of Influential Observation in Linear Regression. *Technometrics* **1977**, *19* (1), 15−18.
(20) Cook, R. D. Influential Observations in Linear Regression. *J. Am. Stat. Assoc.* **1979**, *74* (365), 169−174.
(21) Benjamini, Y.; Hochberg, Y. Controlling the False Discovery Rate: A Practical and Powerful Approach to Multiple Testing. *J. R. Stat. Soc. Ser. B* **1995**, *57* (1), 289−300.
(22) Breitling, R.; Armengaud, P.; Amtmann, A.; Herzyk, P. Rank Products: A Simple, yet Powerful, New Method to Detect Differentially Regulated Genes in Replicated Microarray Experiments. *FEBS Lett.* **2004**, *573* (1−3), 83−92.
(23) The Cancer Genome Atlas Network.. Comprehensive Molecular Portraits of Human Breast Tumours. *Nature* **2012**, *490* (7418), 61−70.
(24) Gao, J.; Aksoy, B. A.; Dogrusoz, U.; Dresdner, G.; Gross, B.; Sumer, S. O.; Sun, Y.; Jacobsen, A.; Sinha, R.; Larsson, E.; et al. Integrative Analysis of Complex Cancer Genomics and Clinical Profiles Using the CBioPortal. *Sci. Signaling* **2013**, *6* (269), pl1.
(25) Cerami, E.; Gao, J.; Dogrusoz, U.; Gross, B. E.; Sumer, S. O.; Aksoy, B. A.; Jacobsen, A.; Byrne, C. J.; Heuer, M. L.; Larsson, E.; et al. The CBio Cancer Genomics Portal: An Open Platform for Exploring Multidimensional Cancer Genomics Data. *Cancer Discovery* **2012**, *2* (5), 401−404.
(26) Curtis, C.; Shah, S. P.; Chin, S. F.; Turashvili, G.; Rueda, O. M.; Dunning, M. J.; Speed, D.; Lynch, A. G.; Samarajiwa, S.; Yuan, Y.; et al. The Genomic and Transcriptomic Architecture of 2,000 Breast Tumours Reveals Novel Subgroups. *Nature* **2012**, *486* (7403), 346−352.
(27) Sobin, L. H.; Gospodarowicz, M. K.; Wittekind, C.; International Union Against Cancer. *TNM Classification of Malignant Tumours*, 7th ed.; Wiley-Blackwell: Chichester, West Sussex, U.K., 2009.
(28) R Development Core Team. *R: A Language and Environment for Statistical Computing*; R Foundation for Statistical Computing, 2013.
(29) Weidemann, A.; Johnson, R. S. Biology of HIF-1α. *Cell Death Differ.* **2008**, *15* (4), 621−627.
(30) Liu, W.; Shen, S.-M.; Zhao, X.-Y.; Chen, G.-Q. Targeted Genes and Interacting Proteins of Hypoxia Inducible Factor-1. *Int. J. Biochem. Mol. Biol.* **2012**, *3* (2), 165−178.
(31) Koh, M. Y.; Powis, G. Passing the Baton: The HIF Switch. *Trends Biochem. Sci.* **2012**, *37* (9), 364−372.
(32) Neermann, J.; Wagner, R. Comparative Analysis of Glucose and Glutamine Metabolism in Transformed Mammalian Cell Lines, Insect and Primary Liver Cells. *J. Cell. Physiol.* **1996**, *166* (1), 152−169.
(33) Luo, W.; Hu, H.; Chang, R.; Zhong, J.; Knabel, M.; O'Meally, R.; Cole, R. N.; Pandey, A.; Semenza, G. L. Pyruvate Kinase M2 Is a PHD3-Stimulated Coactivator for Hypoxia-Inducible Factor 1. *Cell* **2011**, *145* (5), 732−744.
(34) Azoitei, N.; Becher, A.; Steinestel, K.; Rouhi, A.; Diepold, K.; Genze, F.; Simmet, T.; Seufferlein, T. PKM2 Promotes Tumor Angiogenesis by Regulating HIF-1α through NF-KB Activation. *Mol. Cancer* **2016**, *15*, 3.
(35) Williams, A. L.; Khadka, V.; Tang, M.; Avelar, A.; Schunke, K. J.; Menor, M.; Shohet, R. V. HIF1Mediates a Switch in Pyruvate Kinase Isoforms after Myocardial Infarction. *Physiol. Genomics* **2018**, *50* (7), 479−494.
(36) Ino, Y.; Yamazaki-Itoh, R.; Oguro, S.; Shimada, K.; Kosuge, T.; Zavada, J.; Kanai, Y.; Hiraoka, N. Arginase II Expressed in Cancer-Associated Fibroblasts Indicates Tissue Hypoxia and Predicts Poor Outcome in Patients with Pancreatic Cancer. *PLoS One* **2013**, *8* (2), e55146.
(37) Piret, J.-P.; Mottet, D.; Raes, M.; Michiels, C. CoCl2, a Chemical Inducer of Hypoxia-Inducible Factor-1, and Hypoxia Reduce Apoptotic Cell Death in Hepatoma Cell Line HepG2. *Ann. N. Y. Acad. Sci.* **2002**, *973*, 443−447.
(38) Masoud, G. N.; Li, W. HIF-1α Pathway: Role, Regulation and Intervention for Cancer Therapy. *Acta Pharm. Sin. B* **2015**, *5* (5), 378−389.
(39) Ouiddir, A.; Planès, C.; Fernandes, I.; VanHesse, A.; Clerici, C. Hypoxia Upregulates Activity and Expression of the Glucose Transporter GLUT1 in Alveolar Epithelial Cells. *Am. J. Respir. Cell Mol. Biol.* **1999**, *21* (6), 710−718.
(40) Hayashi, M.; Sakata, M.; Takeda, T.; Yamamoto, T.; Okamoto, Y.; Sawada, K.; Kimura, A.; Minekawa, R.; Tahara, M.; Tasaka, K.; et al. Induction of Glucose Transporter 1 Expression through Hypoxia-Inducible Factor 1alpha under Hypoxic Conditions in Trophoblast-Derived Cells. *J. Endocrinol.* **2004**, *183* (1), 145−154.
(41) Semenza, G. L. HIF-1 Mediates Metabolic Responses to Intratumoral Hypoxia and Oncogenic Mutations. *J. Clin. Invest.* **2013**, *123* (9), 3664−3671.
(42) Iyer, N. V.; Kotch, L. E.; Agani, F.; Leung, S. W.; Laughner, E.; Wenger, R. H.; Gassmann, M.; Gearhart, J. D.; Lawler, A. M.; Yu, A. Y.; et al. Cellular and Developmental Control of O2 Homeostasis by Hypoxia-Inducible Factor 1 Alpha. *Genes Dev.* **1998**, *12* (2), 149−162.
(43) Semenza, G. L.; Jiang, B. H.; Leung, S. W.; Passantino, R.; Concordet, J. P.; Maire, P.; Giallongo, A. Hypoxia Response Elements in the Aldolase A, Enolase 1, and Lactate Dehydrogenase A Gene Promoters Contain Essential Binding Sites for Hypoxia-Inducible Factor 1. *J. Biol. Chem.* **1996**, *271* (51), 32529−32537.
(44) Doherty, J. R.; Cleveland, J. L. Targeting Lactate Metabolism for Cancer Therapeutics. *J. Clin. Invest.* **2013**, *123* (9), 3685−3692.

DOI: 10.1021/acs.jproteome.8b00944
J. Proteome Res. 2019, 18, 1352−1362

(45) Feron, O. Pyruvate into Lactate and Back: From the Warburg Effect to Symbiotic Energy Fuel Exchange in Cancer Cells. *Radiother. Oncol.* **2009**, *92* (3), 329−333.
(46) Le, A.; Cooper, C. R.; Gouw, A. M.; Dinavahi, R.; Maitra, A.; Deck, L. M.; Royer, R. E.; Vander Jagt, D. L.; Semenza, G. L.; Dang, C. V. Inhibition of Lactate Dehydrogenase A Induces Oxidative Stress and Inhibits Tumor Progression. *Proc. Natl. Acad. Sci. U. S. A.* **2010**, *107* (5), 2037−2042.
(47) Kim, J.; Tchernyshyov, I.; Semenza, G. L.; Dang, C. V. HIF-1-Mediated Expression of Pyruvate Dehydrogenase Kinase: A Metabolic Switch Required for Cellular Adaptation to Hypoxia. *Cell Metab.* **2006**, *3* (3), 177−185.
(48) Martin-Rufian, M.; Nascimento-Gomes, R.; Higuero, A.; Crisma, A. R.; Campos-Sandoval, J. A.; Gomez-Garcia, M. C.; Cardona, C.; Cheng, T.; Lobo, C.; Segura, J. A.; et al. Both GLS Silencing and GLS2 Overexpression Synergize with Oxidative Stress against Proliferation of Glioma Cells. *J. Mol. Med.* **2014**, *92* (3), 277−290.
(49) Mayers, J. R.; Vander Heiden, M. G. Famine versus Feast: Understanding the Metabolism of Tumors in Vivo. *Trends Biochem. Sci.* **2015**, *40* (3), 130−140.
(50) Rockwell, S.; Dobrucki, I. T.; Kim, E. Y.; Marrison, S. T.; Vu, V. T. Hypoxia and Radiation Therapy: Past History, Ongoing Research, and Future Promise. *Curr. Mol. Med.* **2009**, *9* (4), 442−458.
(51) Doktorova, H.; Hrabeta, J.; Khalil, M. A.; Eckschlager, T. Hypoxia-Induced Chemoresistance in Cancer Cells: The Role of Not Only HIF-1. *Biomed. Pap.* **2015**, *159* (2), 166−177.
(52) Muz, B.; de la Puente, P.; Azab, F.; Azab, A. K. The Role of Hypoxia in Cancer Progression, Angiogenesis, Metastasis, and Resistance to Therapy. *Hypoxia* **2015**, *3*, 83−92.
(53) Cluntun, A. A.; Lukey, M. J.; Cerione, R. A.; Locasale, J. W. Glutamine Metabolism in Cancer: Understanding the Heterogeneity. *Trends in Cancer* **2017**, *3* (3), 169−180.
(54) von Minckwitz, G.; Eidtmann, H.; Rezai, M.; Fasching, P. A.; Tesch, H.; Eggemann, H.; Schrader, I.; Kittel, K.; Hanusch, C.; Kreienberg, R.; et al. Neoadjuvant Chemotherapy and Bevacizumab for HER2-Negative Breast Cancer. *N. Engl. J. Med.* **2012**, *366* (4), 299−309.
(55) Harrison, H.; Rogerson, L.; Gregson, H. J.; Brennan, K. R.; Clarke, R. B.; Landberg, G. Contrasting Hypoxic Effects on Breast Cancer Stem Cell Hierarchy Is Dependent on ER-α Status. *Cancer Res.* **2013**, *73* (4), 1420−1433.
(56) Ueda, S.; Saeki, T.; Osaki, A.; Yamane, T.; Kuji, I. Bevacizumab Induces Acute Hypoxia and Cancer Progression in Patients with Refractory Breast Cancer: Multimodal Functional Imaging and Multiplex Cytokine Analysis. *Clin. Cancer Res.* **2017**, *23* (19), 5769−5778.
(57) Timmerman, L. A.; Holton, T.; Yuneva, M.; Louie, R. J.; Padró, M.; Daemen, A.; Hu, M.; Chan, D. A.; Ethier, S. P.; van 't Veer, L. J.; et al. Glutamine Sensitivity Analysis Identifies the XCT Antiporter as a Common Triple-Negative Breast Tumor Therapeutic Target. *Cancer Cell* **2013**, *24* (4), 450−465.
(58) Gross, M. I.; Demo, S. D.; Dennison, J. B.; Chen, L.; Chernov-Rogan, T.; Goyal, B.; Janes, J. R.; Laidig, G. J.; Lewis, E. R.; Li, J.; et al. Antitumor Activity of the Glutaminase Inhibitor CB-839 in Triple-Negative Breast Cancer. *Mol. Cancer Ther.* **2014**, *13* (4), 890−901.
(59) Budczies, J.; Pfitzner, B. M.; Gyorffy, B.; Winzer, K. J.; Radke, C.; Dietel, M.; Fiehn, O.; Denkert, C. Glutamate Enrichment as New Diagnostic Opportunity in Breast Cancer. *Int. J. Cancer* **2015**, *136* (7), 1619−1628.
(60) Yuneva, M.; Zamboni, N.; Oefner, P.; Sachidanandam, R.; Lazebnik, Y. Deficiency in Glutamine but Not Glucose Induces MYC-Dependent Apoptosis in Human Cells. *J. Cell Biol.* **2007**, *178* (1), 93−105.
(61) Wise, D. R.; DeBerardinis, R. J.; Mancuso, A.; Sayed, N.; Zhang, X.-Y.; Pfeiffer, H. K.; Nissim, I.; Daikhin, E.; Yudkoff, M.; McMahon, S. B.; et al. Myc Regulates a Transcriptional Program That Stimulates Mitochondrial Glutaminolysis and Leads to Glutamine Addiction. *Proc. Natl. Acad. Sci. U. S. A.* **2008**, *105* (48), 18782−18787.
(62) Rofstad, E. K.; Galappathi, K.; Mathiesen, B.; Ruud, E.-B. M. Fluctuating and Diffusion-Limited Hypoxia in Hypoxia-Induced Metastasis. *Clin. Cancer Res.* **2007**, *13* (7), 1971−1978.
(63) Kitajima, S.; Lee, K. L.; Hikasa, H.; Sun, W.; Huang, R. Y.-J.; Yang, H.; Matsunaga, S.; Yamaguchi, T.; Araki, M.; Kato, H.; et al. Hypoxia-Inducible Factor-1α Promotes Cell Survival during Ammonia Stress Response in Ovarian Cancer Stem-like Cells. *Oncotarget* **2017**, *8* (70), 114481−114494.

DOI: 10.1021/acs.jproteome.8b00944
J. Proteome Res. 2019, 18, 1352−1362